**SUPPLEMENTARY MATERIAL**

**Supplementary Table 1**. The central helix of complexin is slightly differently anchored to the SNARE complex. The displacement for each Cα atom between the post-fusion and pre-fusion structure is listed.

| CPXcen Cα | displacement [Å] post- vs. pre-fusion |
|---|---|
| 59 | 2.6 |
| 60 | 1.5 |
| 61 | 1.2 |
| 62 | 1.1 |
| 63 | 0.9 |
| 64 | 0.5 |
| 65 | 0.7 |
| 66 | 1.0 |
| 67 | 0.5 |
| 68 | 0.4 |
| 69 | 0.4 |
| 70 | 0.3 |

**Supplementary Table 2**. The CPX helix twisted differently in the post- and pre-fusion structure. Peptide angles of the CPX region linking the central and accessory helix are listed.

| CPX position | Post-fusion | | Pre-fusion | | Difference | |
|---|---|---|---|---|---|---|
| | phi [°] | psi [°] | phi [°] | psi [°] | phi [°] | psi [°] |
| 45 | -77.4 | -35.2 | -83.4 | -36.1 | 6.0 | 0.9 |
| 46 | -63.1 | -27.8 | -72.3 | -31.8 | 9.2 | 4.0 |
| 47 | -86.1 | -35.4 | -75.3 | -49.5 | -10.8 | 14.1 |
| 48 | -65.4 | -39.4 | -54.2 | -31.6 | -11.2 | -7.8 |
| 49 | -68.7 | -30.4 | -69.1 | -43.4 | 0.4 | 13.0 |
| 50 | -73.3 | -43.5 | -65.9 | -41.7 | -7.4 | -1.8 |
| 51 | -64.9 | -26.0 | -62.3 | -38.7 | -2.6 | 12.7 |
| 52 | -90.0 | -19.9 | -68.1 | -33.2 | -21.9 | 13.3 |
| 53 | -78.2 | -35.6 | -63.4 | -45.4 | -14.8 | 9.8 |
| 54 | -68.3 | -35.9 | -73.3 | -35.0 | 5.0 | -0.9 |
| 55 | -65.2 | -44.9 | -66.3 | -40.9 | 1.1 | -4.0 |
| 56 | -59.5 | -47.4 | -54.8 | -54.8 | -4.7 | 7.4 |
| 57 | -58.2 | -43.9 | -54.2 | -40.6 | -4.0 | -3.3 |
| 58 | -63.1 | -33.9 | -82.4 | -14.2 | 19.3 | -19.7 |
| average | -70.1 | -35.7 | -67.5 | -38.4 | -2.6 | 2.7 |

**Supplementary Table 3:** FRET distances were determined from quenching of donor fluorescence between SNAP25 and CPX when bound to SNARE complexes in post-fusion (VAMP2) or pre-fusion (VAMP2-Δ60, VAMP2-4X) conformation. Error bars refer to n = 4-6 independent experiments. Values measured in the respective crystal structures are given for comparison.

| | **Distance* SNAP25-193 to** | |
|---|---|---|
| | CPX-38 [Å] | CPX-31 [Å] |
| **FRET measurements** | | |
| VAMP2 (25-96) | 20 ± 1 | 27 ± 1 |
| VAMP2-Δ60 (29-60) | 34 ± 1 | 42 ± 1 |
| VAMP2-4X (25-96; L70D,A74R,A81D,L84D) | 33 ± 1 | 38 ± 1 |
| **Measured in crystal structure** | | |
| post-fusion (PDB 1KIL) | 18 | 24 |
| pre-fusion (C2 crystal form) | 28 | 38 |

* Error bars reflect the reproducibility of the spectra rather than accuracy of the distance measurements.

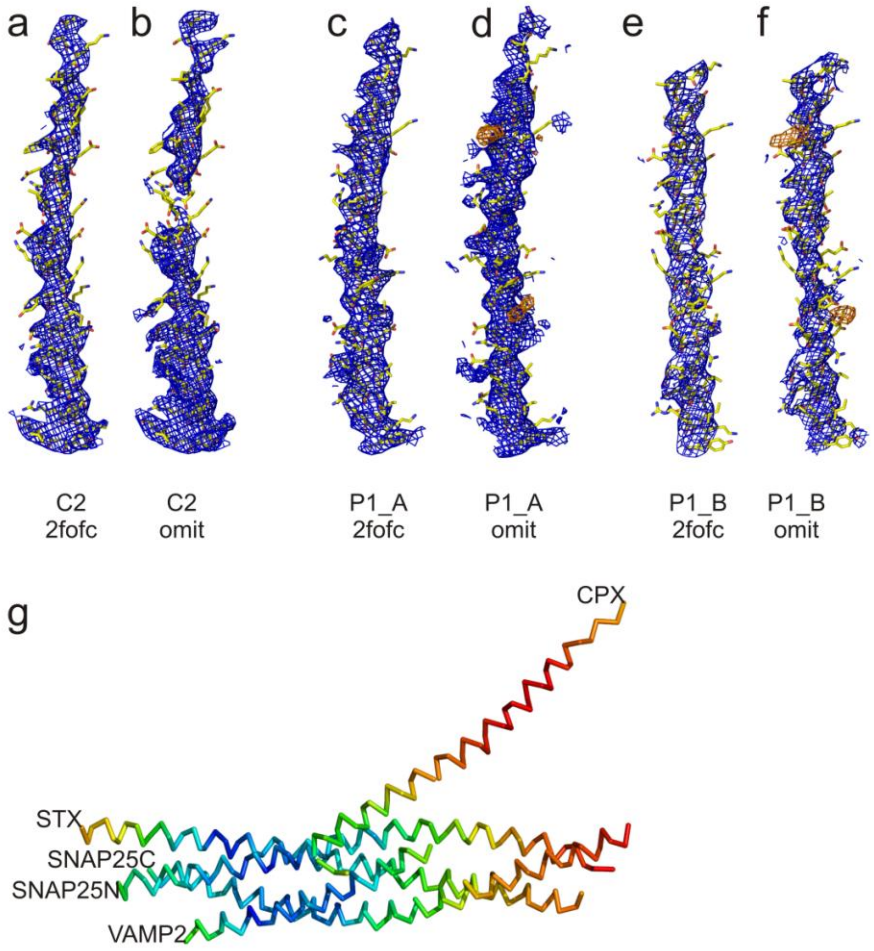


**Supplementary Figure 1**. Electron density for CPX contoured at 1σ. (**a**) Weighted 2fo-fc electron density after refinement and (**b**) composite simulated annealed omit map for CPX in the C2 crystal form. (**c**) Weighted 2fo-fc electron density after refinement (**d**) and four-fold averaged composite simulated annealed omit map for CPX-F34M in binding mode A of the P1 crystal form. (**e**) Weighted 2fo-fc electron density after refinement (**f**) and four-fold averaged composite simulated annealed omit map for CPX-F34M in binding mode B of the P1 crystal form. There are two binding modes for $CPX_{acc}$-F34M and the t-SNARE groove in the P1 crystal form, "A" and "B". CPX and especially its accessory helix have high B-factors, and as seen in (a-f), solvent-exposed side-chains are not well ordered. We therefore used selenomethionine-substituted forms of CPX to confirm the sequence register. The anomalous difference maps used to located the positions of M55 and M34 are shown in orange in (**d**) and (**f**) and are contoured at 3.5 σ. (**g**) B-factor plot of CPX–SNARE complex in rainbow color scheme (blue to red, 17-185 $Å^2$).

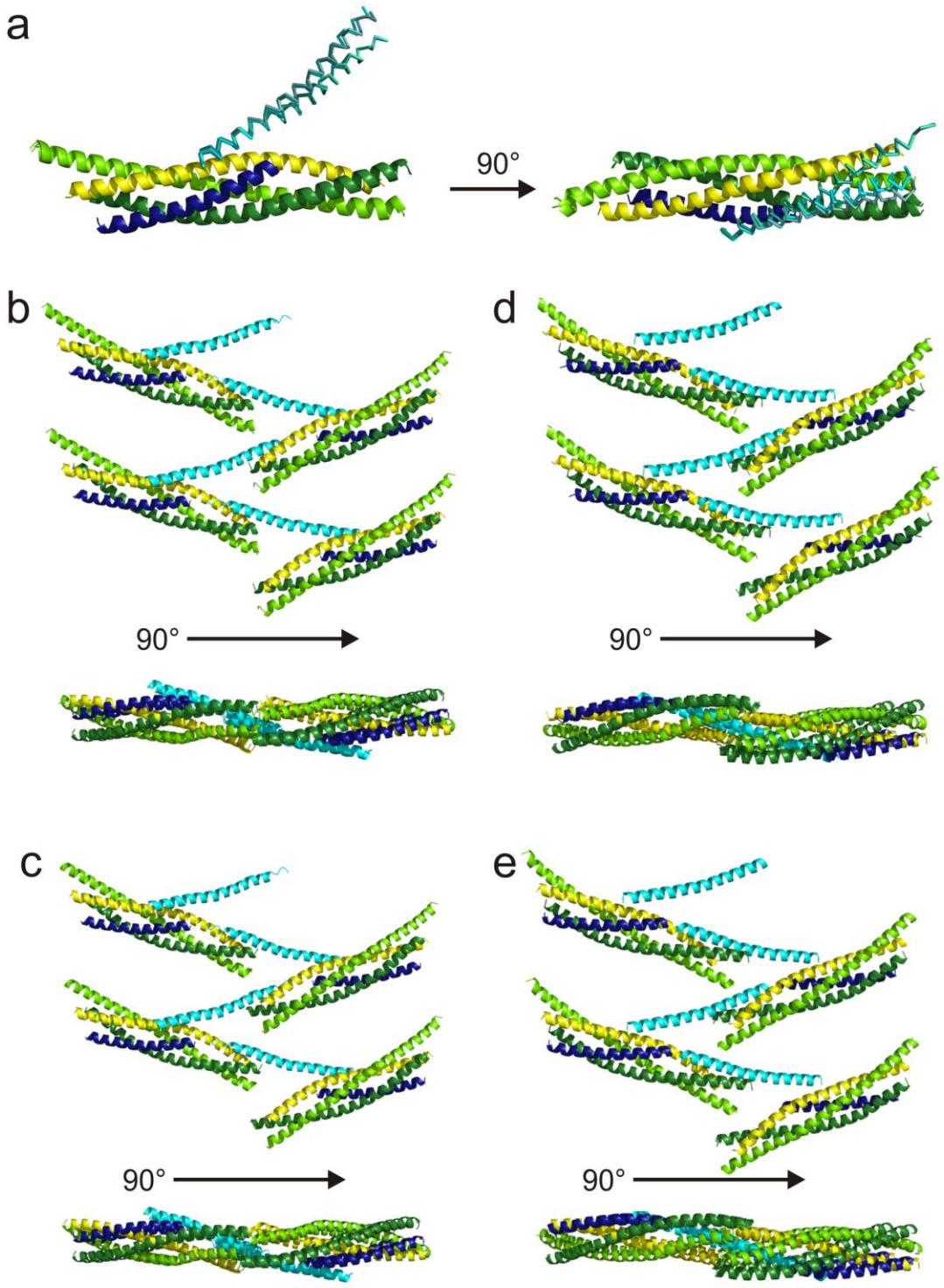


**Supplementary Figure 2**. Zig-zag arrays in the P1 crystal form. (**a**) Superposition of CPX–SNARE complexes constituting four crystallographically distinct zig-zag arrangements in the P1 crystal form. (**b**)-(**e**) Top and side view of the four different lattices in the P1 crystal form.

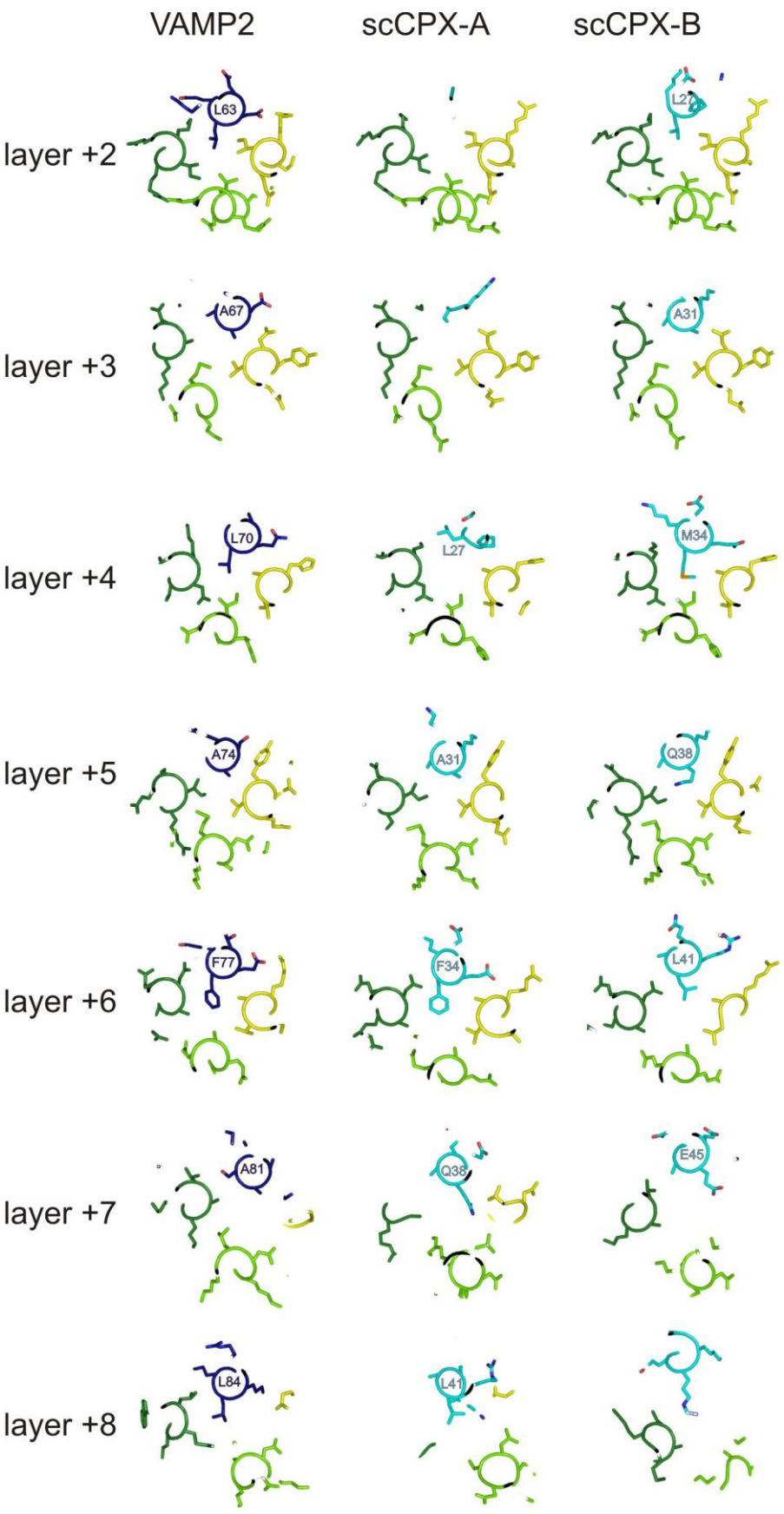


**Supplementary Figure 3.** Comparison of the hydrophobic layer interactions of the t-SNARE groove with VAMP2 (left panels), CPX in binding mode A (middle panels) and in binding mode B (right panels).

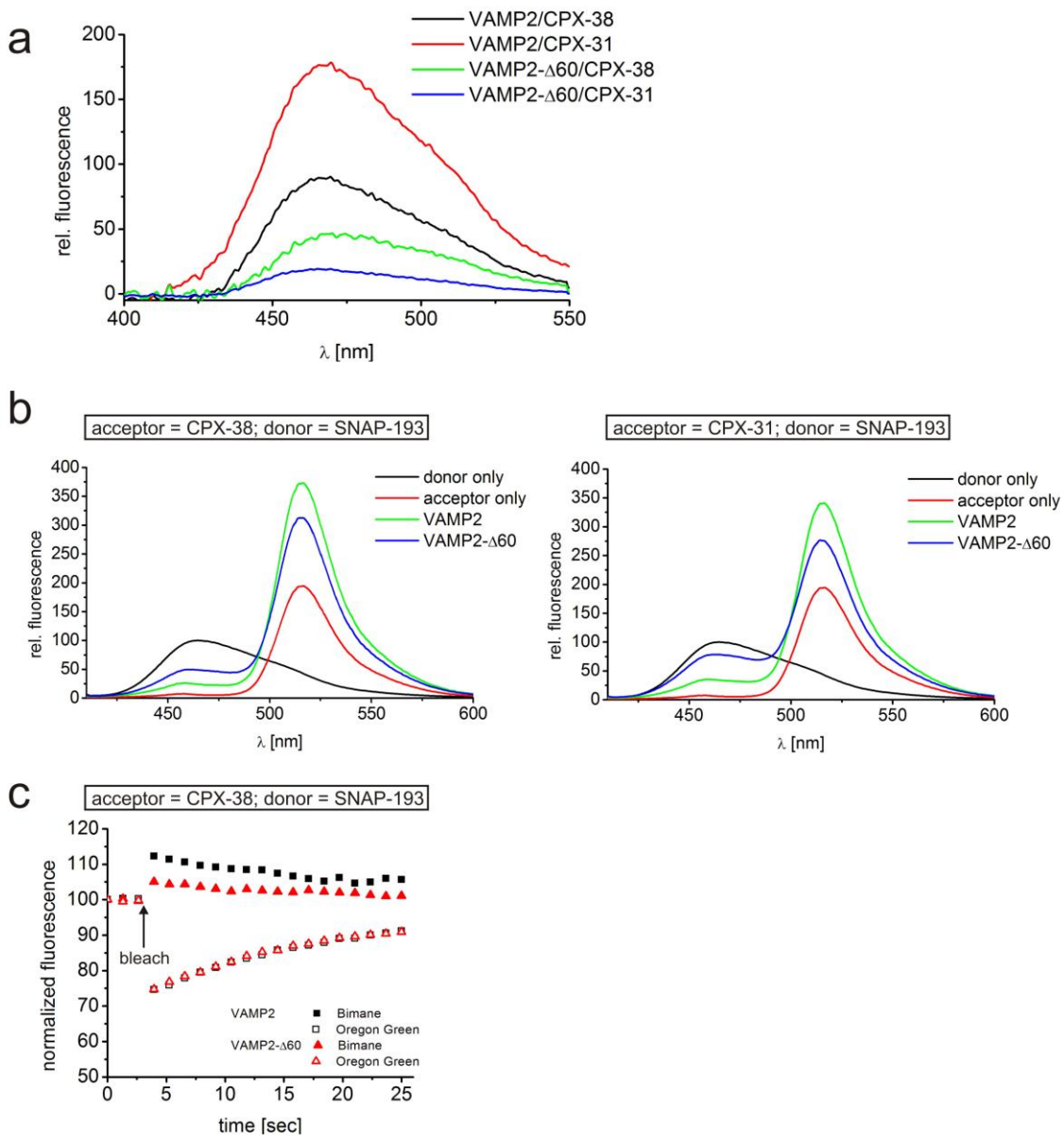


**Supplementary Figure 4.** (**a**) Increase in the acceptor (Bimane) signal correlates with quenching of the donor (Stilbene) fluorescence confirming FRET. Acceptor (Bimane) emission was extracted from the Stilbene or Bimane emission scans by subtracting the donor and buffer contributions. The corrected acceptor emission was then normalized with maximum acceptor fluorescence when excited at acceptor excitation wavelength (396 nm). We observe more FRET with the VAMP2 (residues 25-96) than with VAMP2-Δ60 (residues 25-60), with both CPX labeled on 38 (black vs. green, respectively) and 31 (red vs. blue, respectively) which shows that the $CPX_{acc}$ helix is further away from the SNAREpin in the pre-fusion (VAMP2-Δ60) complex than the post-fusion VAMP2 (residues 25-96) complex. The acceptor fluorescence increase qualitatively matches the

donor-quenching data except for CPX labeled at position 38 in the CPX–SNARE complex containing VAMP2. However, the acceptor emission is 1/3 weaker in this complex compared to the other CPX–SNARE complexes, even though the excitation properties are unaffected. This means the local environment possibly affects the acceptor emission in this case and could explain the anomalous behavior. (**b**) Fluorescence emission spectra of Bimane alone (black), only Oregon green (red), and Bimane or Oregon labeled CPX–SNARE complex containing VAMP2 (residues 25-96, green), VAMP2-Δ60 (residues 25-60, blue) excited at 396 nm. SNAP25 D193C was labeled with donor, Bimane, and CPX was labeled with acceptor, Oregon green 488, at positions 38 (left panel) or 31 (right panel). The FRET measurements from this FRET pair are in good agreement with the results obtained with the Stilbene or Bimane FRET pair, confirming that the $CPX_{acc}$ helix bends away from the SNAREs in the truncated SNARE complex compared to the fully-zippered SNARE complex. (**c**) Bleaching of acceptor (Oregon green) fluorescence results in donor (Bimane) fluorescence increase demonstrating FRET. Fluorescence recovery (FRAP) experiments were done on Bimane or Oregon labeled CPX–SNARE complexes containing VAMP2 (residues 25-96, black) or VAMP2-Δ60 (residues 25-60, red) in a Leica SP5 confocal setup. The acceptor fluorescence was bleached using a 488 nm laser and the fluorescence recovery was recorded in two different channels set at 440-480 nm (Bimane, filled symbols) and 500-540 nm (Oregon green, open symbols) respectively. The fluorescence intensity normalized with respect to the pre-bleach fluorescence is shown above. There is an increase of the donor fluorescence after bleaching of the acceptor and the effect is larger for VAMP2 compared to VAMP2-Δ60. This means $CPX_{acc}$ helix is closer to the SNAREpin in the CPX–SNARE complex containing VAMP2 than in VAMP2-Δ60 complex corroborating our previous results.

**Supplementary Methods**

**Protein Expression, Purification and Complex Assembly.** Recombinant fusion proteins were expressed in *E.coli* BL21 (DE3) cells by induction with 0.5 mM IPTG for 4 h at 37 °C. The constructs used for crystallization are GST-PreScission-VAMP2Δ60 (containing human VAMP2 residues 29-60), GST-TEV-syntaxin1A (containing rat syntaxin1a residues 191-253), oligohistidine-MBP-Thrombin-SNAP25N (containing human SNAP25A residues 7-82 and a C-terminal tryptophan), GST-TEV-SNAP25C (containing human SNAP25A residues 141-203) and GST-PreScission-CPX (containing human complexin1 residues 26-83 with the following "superclamp" mutations: D27L, E34F, R37A). To make CPX-L27M and CPX-F34M, positions 27 or 34 of CPX were mutated to methionine using QuikChange mutagenesis (Stratagene).

Cells were harvested and resuspended in buffer S (140 mM NaCl, 1 mM DTT, 20 mM Tris pH 7.5) supplemented with protease inhibitors (Complete EDTA-free, Roche), DNaseI (Sigma) and lysozyme (American Bioanalytical), then lysed using a cell disruptor (Avestin). Proteins were purified with either glutathione-Sepharose (GE) or Ni-NTA-agarose (Qiagen) resin according to manufacturers' instructions. Tags were cleaved with TEV, PreScission or thrombin (Sigma) protease overnight at 4 °C. The proteins were collected, concentrated and purified by size exclusion chromatography on a HiLoad Superdex 75 (16/60, GE Healthcare) column equilibrated with buffer S. Selenomethionine substituted CPX-L27M and CPX-F34M were expressed according to Doublie [1] and purified as described above.

To reconstitute the truncated SNARE complex, VAMP2-Δ60, SNAP25C, SNAP25N and synatxin1 were mixed at 1:1:1:1 molar ration and incubated for 2 h before gel filtration on a HiLoad Superdex 75 (16/60, GE Healthcare) column equilibrated with buffer S. CPX was added to the truncated SNARE complex at 1.2 molar excess and incubated over night. The sample was supplemented with imidazole (20 mM final concentration) and passed over 0.5 ml Ni-NTA resin three times to remove TEV and PreScission proteases, which are oligohistidine tagged. The mixture was loaded on a HiLoad Superdex 75 (16/60, GE Healthcare) column equilibrated with buffer S, and peak fractions were pooled and concentrated to ~10 mg $ml^{-1}$ for crystallization.

**Isothermal Titration Calorimetry (ITC) analysis**

Syntaxin1A, SNAP25C, SNAP25N and VAMP2-Δ60 were mixed together at a 1:1.2:1.2:1.2 molar ratio and incubated at 4°C overnight to form the SNARE-Δ60 complex. Before ITC experiments, SNARE-Δ60 and CPX variants (CPX48-134, wtCPX, scCPX, ncCPX) were purified by gel filtration using a HiLoad Superdex 75 column (GE Healthcare Life Sciences) and PBS (phosphate buffered saline, pH 7.4: 137 mM NaCl, 3 mM KCl, 10 mM sodium phosphate dibasic, 2 mM potassium phosphate monobasic) with 0.25 mM TCEP as the running buffer, respectively. Peak fractions were pooled and concentrated. CPX 48-134 was added into SNARE-Δ60 at about 1.5:1 molar ratio and incubate overnight at 4°C to form blocked SNARE-Δ60. CPX variants and blocked SNARE-Δ60 were then dialyzed in the same flask against 3 liters of PBS buffer with 0.25 mM TCEP for 4 hours at 4°C and then dialyzed against another 3 liters of fresh PBS buffer with 0.25 mM TCEP overnight at 4°C. The concentrations of dialyzed proteins were determined by using the Thermo Scientific Pierce Bicinchoninic Acid (BCA) protein assay kit with BSA as the standard and/or Bradford assay.

ITC experiments were performed on a Microcal ITC200 instrument. Typically, about 200 μL of blocked SNARE solution (10 to 30 μM) was loaded into the sample cell and about 40 μL of CPX solution (200 to 600 μM) was loaded into the syringe. An initial 0.2 μL injection was followed by several injections of constant volume. 180-second equilibration time was used after each injection to ensure complete binding. The heat change from each injection was integrated, and then normalized by the moles of CPX in the injection. All ITC experiments were carried out at 37°C and at least twice. Microcal Origin ITC200 software package was used to analyze the titration calorimetric data and obtain the stoichiometric number (*N*), the molar binding enthalpy (*ΔH*), and the association constant ($K_a$). "One-set-of-sites" binding mode was used. The equilibrium dissociation constant ($K_d$), the binding free energy (*ΔG*), and the binding entropy (*ΔS)* were calculated using the thermodynamic equations:

$$K_d = \frac{1}{K_a}$$

$$\Delta G = -RT \ln K_a$$

$$\Delta G = \Delta H - T\Delta S$$

Samples as used in the ITC experiments were re-analyzed by size exclusion chromatography using the HiLoad Superdex 75 column to control that VAMP-60 does not dissociate from the t-SNARE complex during the measurements.

**FRET analysis.** Positions D193 on SNAP25 and Q38 or A31 on CPX (hCpx1 residues1-134 carrying superclamp mutations D27L, E34F and R37A was used in all FRET experiments) were mutated into cysteines using the Stratagene QuikChange Kit. SNAP25 D193C was labeled with the donor probe, Stilbene (4-acetamido-4'-((iodoacetyl)amino)-stilbene-2,2'-disulfonic acid, disodium salt, Invitrogen) and either CPX Q38C or A31C was labeled with the acceptor Bimane (Monochlorobimane, Invitrogen). Stilbene has improved solubility compared to the established FRET dye Pyrene, and in conjunction with Bimane, it can be used to measure small changes at small distances. The proteins were labeled using 10X molar excess of dye overnight at 4°C in 50 mM Tris Buffer, pH 7.4, containing 150 mM NaCl, 10 % Glycerol and 1 mM TCEP. Following overnight incubation at 4°C, the excess dye was separated from the labeled proteins using a NAP desalting column (GE Healthcare). The labeling efficiency was calculated using $\varepsilon_{335}$ = 35,000 L $m^{-1}cm^{-1}$ for Stilbene and $\varepsilon_{396}$ = 5,300 L $m^{-1}cm^{-1}$ for Bimane, and the protein concentration was measured by Bradford assay using BSA as the standard. Typically, the labeling efficiency was >90% for Stilbene-SNAP25 and ~75% for Bimane-CPX. The double-labeled CPX–SNARE complexes were assembled overnight at 4°C and purified by gel-filtration on a Superdex 75 (10/30, GE Healthcare) gel filtration column. All fluorescence data were obtained on a Perkin-Elmer LS55 luminescence spectrometer operating at 25°C. Excitation and emission slits of 5 nm were used in all measurements. Fluorescence emission spectra were measured over the range of 350-550 nm with the excitation wavelength set at 335 nm. Background fluorescence from the buffer was subtracted to calculate the reported fluorescence values. The donor probe concentration was adjusted to 2 µM in all samples. Fluorescence resonance energy transfer (FRET) was used to calculate the distance between the two fluorophores [2]. According to the FRET theory, the efficiency of energy transfer (E) is related to the distance (R) between the two fluorophores by

$$E = R_0^6/(R_0^6 + R^6).$$

$R_0$, the distance at the transfer efficiency equals 50% is given by the following equation:

$$R_0 = 9.78 \cdot 10^3 \left(\kappa^2 \eta^{-4} Q_D J\right)^{1/6}$$

The spectral overlap integral (J) between the donor emission spectrum and acceptor absorbance spectrum was approximated by using the summation

$$J(\lambda) = \int_0^\infty F_D(\lambda)\varepsilon_A(\lambda)\lambda^4 d\lambda \Big/ \int_0^\infty F_D(\lambda) d\lambda$$

Where, $F_d(\lambda)$ and $\varepsilon_A(\lambda)$ represent the fluorescence intensity of the donor and the molar extinction coefficient of the acceptor at the wavelength $\lambda$. The overlap integral was calculated to be 1.34 X $10^{-14}$. The quantum yield ($Q_D$) of the Stilbene-SNAP25 was calculated to be 0.19 using tryptophan in solution ($Q_D$ = 0.14) as the reference[3]. Polarization studies of SNAP25 193-Stilbene, CPX38-Bimane and CPX31-Bimane in both full-length and truncated SNARE complexes gave anisotropy values around 0.1 showing that the FRET probes have isotropic motion, so value of 2/3 was used for orientation factor ($\kappa^2$). The refractive index of the medium ($\eta$) was measured to 1.358. Using these values, $R_0$ for the Stilbene-Bimane FRET pair was calculated to be 27.5 Å.
The energy transfer data were obtained by measuring the change in donor fluorescence (donor quenching) in the presence of the acceptor. The donor fluorescence intensity was measured in the absence ($f_d$) and presence ($f_a$) of acceptor. The efficiency of transfer (E) was calculated using the equation $E = 1- f_a/f_d$. Since the labeling efficiency was not 100%, the observed transfer efficiency ($E_{obs}$) was corrected for the acceptor stoichiometry. The corrected efficiency ($E_{cor}$) is given as $E_{cor} = E_{obs}/f_a$, where $f_a$ is the fraction of assembly with acceptor[2].

**References for Supplementary Material**


1. Doublie, S. Preparation of selenomethionyl proteins for phase determination. *Methods Enzymol* **276**, 523-30 (1997).
2. Lakowicz, J.R. *Principles of fluorescence spectroscopy*, xxvi, 954 p. (Springer, New York ; Berlin, 2006).
3. Wu, P. & Brand, L. Resonance energy transfer: methods and applications. *Anal Biochem* **218**, 1-13 (1994).